

UDK 621

## STRUCTURE AND PROPERTIES OF NANOCRYSTALLINE COMPOSITE MATERIALS

J. Konieczny

L. Dobrzański

Profesor, Dr. hab.

Institute of Engineering Materials  
and Biomaterials,  
Faculty of Mechanical Engineering,  
Silesian University of Technology,  
Gliwice, Poland

*The paper concerns investigation of nanocrystalline composites technology preparation. The composites in the form of rings with rectangular transverse section, and with polymer matrix and nanocrystalline metallic powders fulfillment were made, for obtaining a good ferromagnetic properties. The nanocrystalline ferromagnetic powders were manufactured by mechanical milling of metallic glasses ribbons (after annealing state), and also by mechanical alloying of poor powder components. Generally for investigation, the Fe and Co matrix alloys and thermoplastic and hardening polymers including elastomers were used. Magnetic properties in the form of hysteresis loop were measured. Magnetic properties of composites materials were compared with properties of wound cores of nanocrystalline ribbons and powder cores (rings) solidify by pressing and gluing. Generally powder cores showed lower soft ferromagnetic properties than wound cores of nanocrystalline ribbons, but composites cores showed interesting mechanical properties. The attempt of clarifying this effect was performed. Furthermore, the structure of ribbons and the influence of structure and granulation of powders and their shape on properties of composites were investigated.*

**nanocrystalline composite material, magnetic properties, structure**

**1. Introduction.** Amorphous and nanocrystalline alloys based on cobalt produced by melt spinning technique show excellent soft magnetic properties [1÷3]. This properties and mechanical properties can be improve (change) by typical heat treatment (isothermal heating) [4, 5] or by heat treatment in magnetic field [6].

Unfortunately the nanocrystalline metallic materials obtained directly in the process of the metallic glass crystallization are available mainly in the form of very thin ribbons, which results from the production process (melt spinning) [7, 8].

The nanocrystalline composite materials which may be obtained and used in the powder (loose) state, seems to be a very interesting issue from the point of view of the production technology, processing and application [9÷12].

The production of the soft magnetic powder materials in the high energy ball milling or in the mechanical alloying, enables the scientists to work on the ferromagnetic nanocomposites which dimensions and shape may be formed in various consolidation methods [13-15].

Recently, different consolidation techniques have been reported. However the proposed procedures, like explosive compaction, shock-wave compaction and the static high-pressure compaction with pressures up to 5 GPa are costly and complex [16-19]. To improve the range of applications of powders, we have prepared composite materials made of nanocrystalline powders embedded in polymers.

One should take into account the unfavourable demagnetization effect incase in the magnetically soft powder materials. Saturation is acquired during magnetizing of the

short cylindrical specimen only at the field intensity much higher than in case of the closed toroidal core. The reason for that is that the magnetic field intensity  $H_i$  in a short specimen is lower than the field intensity  $H$  in the entire coil [20, 21]. There is a relationship between the magnetization  $J$  and field intensity, which may be represented in the following form, taking into account the partial demagnetizing conditioned by the specimen shape:

$$J = \mu_0 H \frac{\kappa}{1 + \kappa N}, \quad (1)$$

where:  $N$  — demagnetization coefficient (shape factor);  $\kappa$  — magnetic susceptibility;  $\mu_0$  — induction constant (magnetic permeability of vacuum). Coefficient  $N$  in case of, e.g., cylindrical specimens, is determined mostly by the ratio of specimen length  $l$  to its diameter  $D_p$  [20]:

$$p = \frac{l}{D_p}. \quad (2)$$

The shorter and thicker is the cylindrical bar, the smaller value is acquired by  $p$ , and thus  $N$  coefficient has a bigger value. The weakening demagnetizing field which is developed by the specimen inside itself when it is introduced into the magnetic field with the intensity  $H$  is:

$$H - H_i = H - H \frac{1}{1 + \kappa N} = NH \frac{\kappa}{1 + \kappa N} = N \frac{J}{\mu_0}. \quad (3)$$

The research has revealed that the demagnetization coefficient  $N$  depends also on the material's permeability  $\mu$  and it is the bigger, the bigger is  $\mu$  [20].

The aim of this work is to investigate the structure and magnetic properties and influence of temperature of hot pressing on the magnetic properties of the powder  $\text{Co}_{68}\text{Fe}_4\text{Mo}_1\text{Si}_{13.5}\text{B}_{13.5}$  alloy obtained from the metallic glass in the high energy ball milling process.

**Material and methods.** The investigations were carried out on a  $\text{Co}_{68}\text{Fe}_4\text{Mo}_1\text{Si}_{13.5}\text{B}_{13.5}$  metallic glass in form of 0.025 mm thick and 10.2 mm wide ribbons. A 8000 SPEX CertiPrep Mixer/Mill high energy ball mill was applied to mill the ribbons both in „as quenched“ state and heat treated. The vibration times were 5 and 20 hours. A THERMOLYNE F6020C resistance furnace was used for isothermal soaking of the powder.

The hot pressing process was made on machine „Degussa“ was subjected metallic powder obtained in high energy ball milling amorphous ribbon  $\text{Co}_{68}\text{Fe}_4\text{Mo}_1\text{Si}_{13.5}\text{B}_{13.5}$  by 20 hours. Such away prepared powder was compacted in uniaxial press in vacuum ( $2 \times 10^{-2}$  Tr), in temperature  $800^\circ\text{C}$  as well as  $950^\circ\text{C}$  by 20 minutes, with pressure of stamp the  $P = 15$  MPa.

The X-ray tests were realized with the use of the XRD 7 SEIFERT-FPM diffractometer equipped with the lamp of the cobalt anode of 35 kV voltage and 30 mA filament current was used. Diffraction tests were carried out in the  $2\theta$  angle range from  $40$  to  $120^\circ$  (measurement step  $0.1^\circ$ ). Pulse counting time was 5 s. Sizes of Co- $\beta$  crystallites were determined with Scherrer's method [22]:

$$B = \frac{k\lambda}{d \cos \theta_B}, \quad (4)$$

where:  $d$  — diameter of the crystalline particle;  $B$  — width of the diffraction peak measured at half of its height;  $k$  — coefficient assumed as equal to 1 [16];  $\lambda$  — X-ray radiation wavelength;  $2\theta_B$  — radiation beam diffraction angle corresponding to the Bragg maximum.

Microscope examinations were made on the OPTON DSM 940 electron scanning microscope and the JEOL JEM 200CX electron transmission one and on the LEICA MAEF4A® light microscope using the LEICA® firm computer program which on the dimension measurement of the powder grains was done. Tests of magnetic properties were carried out by the use of Lake Shore's Vibrating Sample Magnetometer VSM model 7307.

**Results and discussion.** The investigated  $\text{Co}_{68}\text{Fe}_4\text{Mo}_1\text{Si}_{13.5}\text{B}_{13.5}$  alloy was delivered in the as quenched state and had the amorphous structure. Broad, diffused rings originating from the amorphous phase are visible in the electron diffraction (Fig.1). No crystalline phase was revealed in the as quenched state and the X-ray diffraction displays the evident wide-angled, diffused spectrum, characteristic for the amorphous state.

The obtained powders have the highest portion of the  $400\div 800$   $\mu\text{m}$  fraction at the beginning stage of milling of the  $\text{Co}_{68}\text{Fe}_4\text{Mo}_1\text{Si}_{13.5}\text{B}_{13.5}$  amorphous alloy. The most probable sizes in the powder grains population (mode) are  $476$   $\mu\text{m}$  for the material obtained after 5 hours of milling. Milling the material for 20 hours causes further size reduction of particles (Fig. 2). The highest portion of  $\sim 15\%$  was found out for particles from the range of  $13\div 18$   $\mu\text{m}$ , the arithmetic average of the powders diameter is  $14.88$   $\mu\text{m}$ .

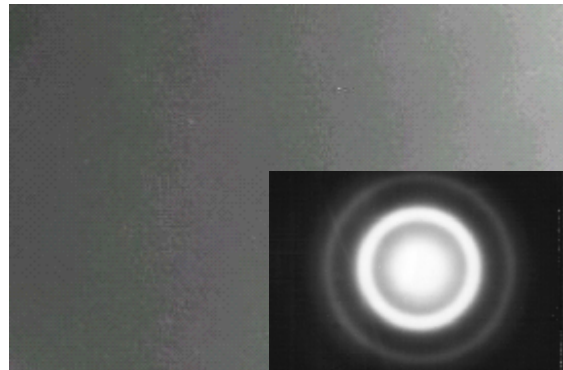


Fig. 1. Amorphous structure of the  $\text{Co}_{68}\text{Fe}_4\text{Mo}_1\text{Si}_{13.5}\text{B}_{13.5}$  alloy, TEM magnification 60000x

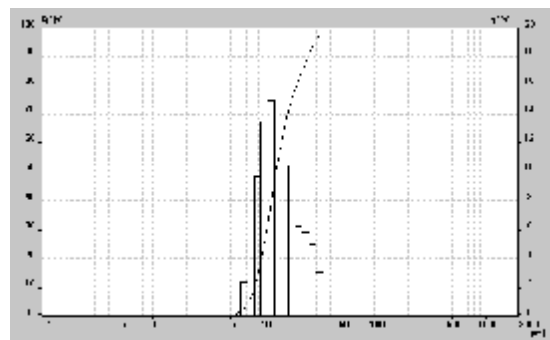


Fig. 2. The cumulative percentage portions curve and the grain size distribution curve for the powder obtained after 20 hours long milling of the  $\text{Co}_{68}\text{Fe}_4\text{Mo}_1\text{Si}_{13.5}\text{B}_{13.5}$  amorphous ribbon of the metallic glass

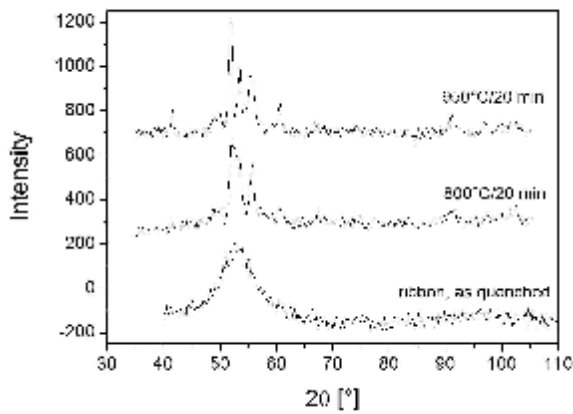


Fig. 3. X-ray diffraction pattern of the  $\text{Co}_{68}\text{Fe}_4\text{Mo}_1\text{Si}_{13.5}\text{B}_{13.5}$  ribbon in as quenched state and powder materials hot pressed in temperature 800 and 950°C in argon atmosphere

On the basis of the analysis of the electron diffraction pattern (Fig. 3) it may be supposed that apart from the stress relaxation, the hot pressing process results in the structural changes which consists of new phase nucleation in higher temperatures. In the X-ray photograph of die stamping obtained in 800°C of hot pressing process the Co- $\alpha$  (111) and (024) with crystallite size suitably 9 and 39 nm, Co- $\beta$  (100), (101) and (110) crystallite size suitably 56, 39 and 11 nm, as well as the  $\text{Co}_3\text{B}$  (021) and (022) phases were identified (Table 1).

In the X-ray diffraction pattern of die stamping obtained in 950°C of hot pressing the Co- $\alpha$  (111) and (024) with crystallite size suitably 20 and 21 nm, Co- $\beta$  (111) and (101) crystallite size suitably 15 and 21 nm, as well as the  $\text{Co}_3\text{B}$  (021) phases were identified (Fig. 3).

The magnetic research of the  $\text{Co}_{68}\text{Mo}_1\text{Fe}_4\text{Si}_{13.5}\text{B}_{13.5}$  powders obtained in the process of milling of the ribbons in the “as quenched” state proved that the process of the high energy ball milling causes significant increase in the coercive force. The powder obtained after 5-hour milling of the amorphous ribbon is characterized by the highest value of the coercive force ( $H_c=159,9$ ). The longer the time of milling

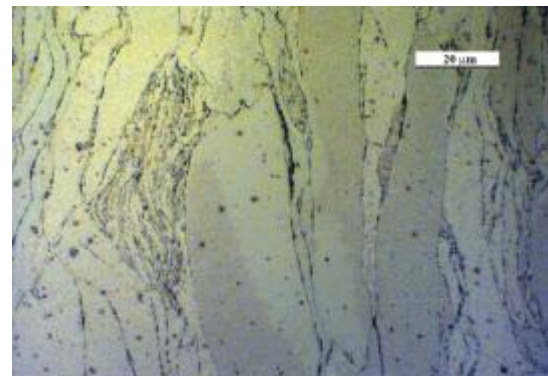
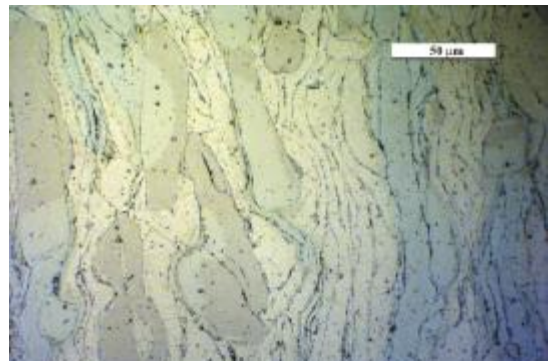


Fig. 4. Structure of composite material obtained in hot pressing process in temperature 800°C

is, the higher the value of the parameter after 20-hour milling  $H_c=1286,6$  A/m.

The longer the milling process, the smaller the value of the saturation of magnetization, which for the powder obtained after 5-hour milling of the amorphous  $\text{Co}_{68}\text{Mo}_1\text{Fe}_4\text{Si}_{13.5}\text{B}_{13.5}$  ribbon amounts to  $B_s=0,63$  T. For the powder obtained in 20-hour milling, the value  $B_s$  equals 0,74 T.

The composite structure is showed in Fig. 4 and Fig. 5, The structure is very similar to schematics of evolution during milling of ductile-brittle combination of powder particles in [23].

Table 1

The phase analysis results for the hot pressed powder  $\text{Co}_{68}\text{Fe}_4\text{Mo}_1\text{Si}_{13.5}\text{B}_{13.5}$  alloy (see Fig. 2)

Hot pressed powder $\text{Co}_{68}\text{Fe}_4\text{Mo}_1\text{Si}_{13.5}\text{B}_{13.5}$ alloy							
950°C/20 minutes				800°C/20 minutes			
2 $\theta$ [°] calculated	2 $\theta$ [°] ICDD	phase	(hkl)	2 $\theta$ [°] calculated	2 $\theta$ [°] ICDD	phase	(hkl)
41,54	41,24	$\text{Co}_2\text{Si}$ (Pbnm)	(111)	52,05	52,50	Co- $\alpha$ (Fm3m)	(111)
48,84	48,96	$\text{Fe}_3\text{B}$ (I-4)	(002)	53,21	53,15	Co- $\beta$ (P63/mmc)	(100)
49,98	50,28	$\text{Co}_2\text{B}$ (I4/mcm)	(221)	55,76	56,24	$\text{Co}_3\text{B}$ (Pbnm)	(021)
52,05	52,50	Co- $\alpha$ (Fm3m)	(111)	60,84	60,94	Co- $\beta$ (P63/mmc)	(101)
53,65	53,15	Co- $\beta$ (P63/mmc)	(100)	60,84	60,33	Co- $\alpha$ (Fm3m)	(024)
55,41	56,24	$\text{Co}_3\text{B}$ (Pbnm)	(021)	67,20	67,90	$\text{Co}_3\text{B}$ (Pbnm)	(022)
60,58	60,94	Co- $\beta$ (P63/mmc)	(101)	91,58	91,10	$\text{Co}_2\text{B}$ (I4/mcm)	(402)
60,84	60,33	Co- $\alpha$ (Fm3m)	(024)	102,64	101,37	Co- $\beta$ (P63/mmc)	(110)
90,97	89,99	$\text{Co}_2\text{B}$ (Pbnm)	(130)				

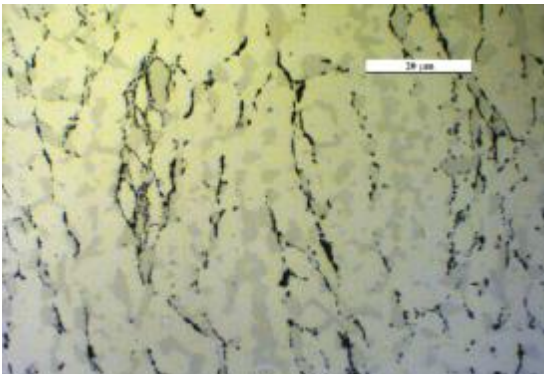
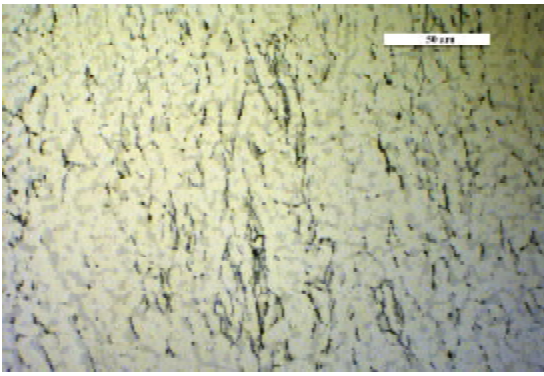


**Fig. 5. Structure of composite material obtained in hot pressing process in temperature 950°C**

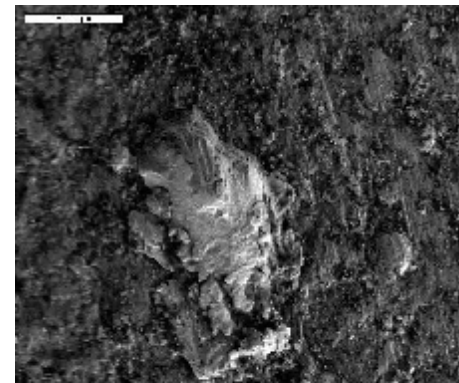
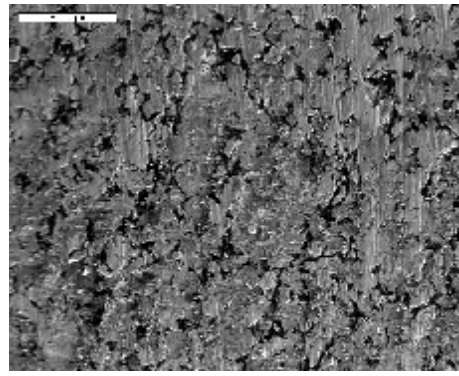


**Fig. 6. The image of  $\text{Co}_{68}\text{Fe}_4\text{Mo}_1\text{Si}_{13.5}\text{B}_{13.5}$  surface structure of die stamping hot pressed in a) 800°C, and b) 950°C per 20 minutes**

The mass density of material of amorphous  $\text{Co}_{68}\text{Mo}_1\text{Fe}_4\text{Si}_{13.5}\text{B}_{13.5}$  ribbon which was the precursor of die stampings carries out  $7.8 \text{ g/cm}^3$ . The mass density of powder after hot pressing in vacuum was calculated, which carries out  $r_{800}=3.789 \text{ g/cm}^3$  for temp.  $800^\circ\text{C}$  and  $r_{950}=4.042 \text{ g/cm}^3$  for temp.  $950^\circ\text{C}$ . The surface structure of die stampings shows on Fig. 6.

The magnetic research of the hot pressed powder  $\text{Co}_{68}\text{Mo}_1\text{Fe}_4\text{Si}_{13.5}\text{B}_{13.5}$  obtained in the process of pressing of the powders proved that the process causes significant increase in the coercive force. The die stamping material obtained after hot pressing in  $800^\circ\text{C}$  per 20 minutes in vacuum from the metallic powder is characterized by the highest value of the coercive force ( $H_c=1363,1 \text{ A/m}$ ). The higher the temperature of pressing is, the higher the value of the parameter after  $950^\circ\text{C}$  pressing  $H_c=3517,0 \text{ A/m}$  (Fig. 7).

A specially significant is the growing value of coercive force  $H_c$  with grooving temperature of hot pressing. The coercive force value increases up to  $950^\circ\text{C}$ . The saturation magnetization  $B_s$  changed too, the value decreases from  $0.74 \text{ T}$  for powder obtained after 20 hours of high energy ball milling to  $0.48 \text{ T}$  for die stamping obtained in  $800^\circ\text{C}$  per 20 minutes and for  $0.52 \text{ T}$  for die stamping obtained in  $950^\circ\text{C}$ .

The lower the temperature of hot pressing, the smaller the value of the saturation of magnetization, which for the die stamping of the powdered  $\text{Co}_{68}\text{Mo}_1\text{Fe}_4\text{Si}_{13.5}\text{B}_{13.5}$  ribbon amounts to  $B_s=0,48 \text{ T}$ . For the die stamping obtained in temperature  $950^\circ\text{C}$ , the value  $B_s$  equals  $0,52 \text{ T}$ . The value of the residual flux density is very low for both pressed materials and  $B_r$  is equal  $0.0124 \text{ T}$  and  $0.0055$  for die stamping obtained respectively at  $800^\circ\text{C}$  and  $950^\circ\text{C}$  (Table 2).

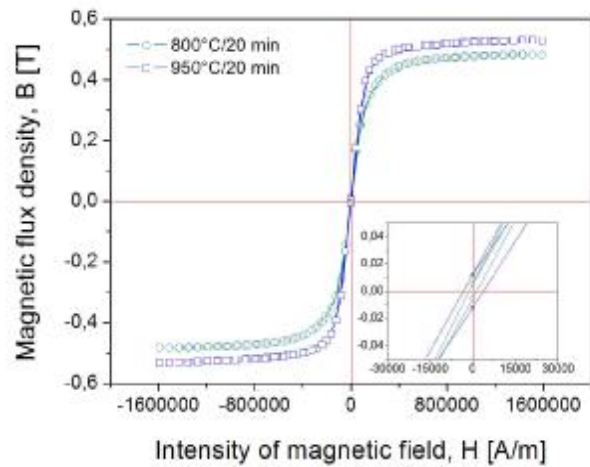


**Fig. 7. Hysteresis loop of the powder of  $\text{Co}_{68}\text{Fe}_4\text{Mo}_1\text{Si}_{13.5}\text{B}_{13.5}$  alloy hot pressed in  $800$  and  $950^\circ\text{C}/20$  minutes**

The silicone matrix polymer composites were made using as filler the powder material obtained by annealing of the  $\text{Co}_{68}\text{Fe}_4\text{Mo}_1\text{Si}_{13.5}\text{B}_{13.5}$  amorphous ribbon for 1 hour at a temperature of  $450^\circ\text{C}$  in the argon atmosphere, and by further milling the ribbon in the SILAME high energy mill for 10 minutes. The powder obtained after annealing the ribbon at  $450^\circ\text{C}$  for 1 hour and milling for 10 minutes was mixed with the silicone polymer (technical all-purpose silicone Technicoll®) with the volume fraction of metallic powder 67, 75, 80, 83 and 86% and further the toroidal cores were formed from the obtained composite slurry, which were then

Table 2

Magnetic properties of powder cores obtained in hot pressing process

Materials	$B_s$ [T]	$H_c$ [A/m]	$B_r$ [T]	$H_{max}$ [T]
as quenched	0,54	15,1	0,26	1000
5h HEBM	0,63	159,9	0,0015	796178
20h HEBM	0,74	1286,6	0,0076	
800°C/20'	0,48	1363,1	0,0124	1592356
950°C/20'	0,53	3517,0	0,0055	

HEBM – High Energy Ball Milling process

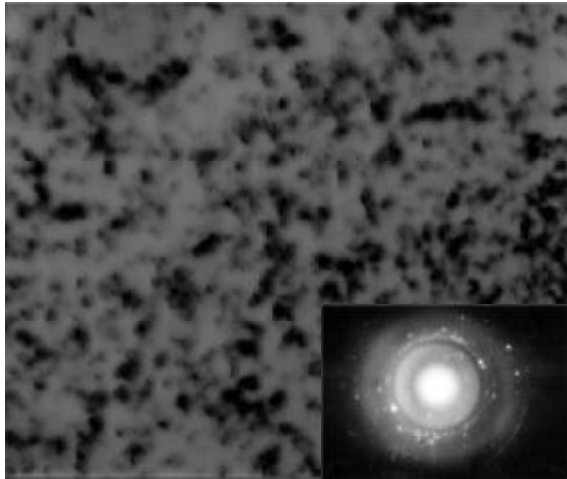


Fig. 8. Structure of ribbon  $Co_{68}Fe_4Mo_1Si_{13.5}B_{13.5}$  alloy after annealing in 450°C/ 1 hour observed in TEM

cured at room temperature for two days. The mass density of composite material with silicon polymer matrix calculated and their values present in table 3.

Observations on the transmission electron microscope (TEM) revealed that combination of the high energy milling and heat treatment carried out even for short periods results in development of the nanocrystalline structure (Fig. 8). This structure differs from the structure obtained by the isothermal annealing of amorphous strips, it is more irregular, and grains present in them are very diversified as regards their shape and sizes. Basing on analysis of the diffraction patterns from the transmission electron microscope the  $Co-\beta$  and  $Co_3B$  cobalt boride phases were revealed in structure of powder obtained after combination of the high energy milling and heat treatment (Fig. 8).

Basing on the microscope examinations it was found out that with the higher content of the  $Co_{68}Fe_4Mo_1Si_{13.5}B_{13.5}$  powder, its particles are homogeneously distributed in the entire silicon matrix. Along with decreasing the powder volume in the composite agglomerations of powder particles occur (Fig. 8).

Tests of magnetic properties revealed that the highest magnetic saturation was characteristic for the composite with the volume fraction of nanocrystalline powder 83% -  $B_s = 0.72$  T. Magnetic saturation values decreased along with the lowering volume fraction of metallic powder in the composite, reaching  $B_s = 0.5$  T (Fig. 9) for the composite with the volume fraction of metallic powder 67%.

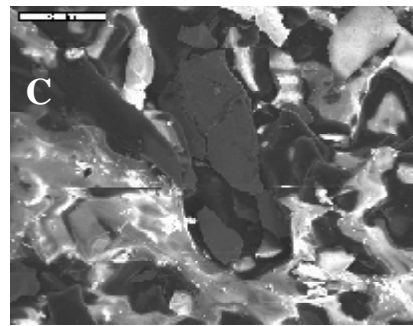
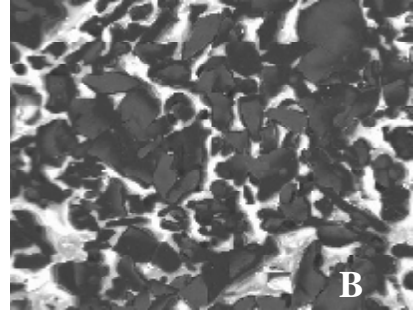
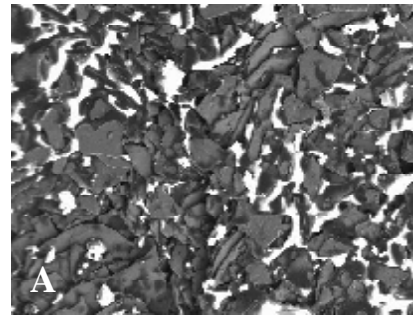


Fig 8. Structures of the nanocrystalline composite material with the silicon matrix reinforced with powder made from the  $Co_{68}Fe_4Mo_1Si_{13.5}B_{13.5}$  alloy with varying the volume fraction of nanocrystalline powder in the SILAME type composite (A) 86, B) 80, C) 75%; electron scanning microscope

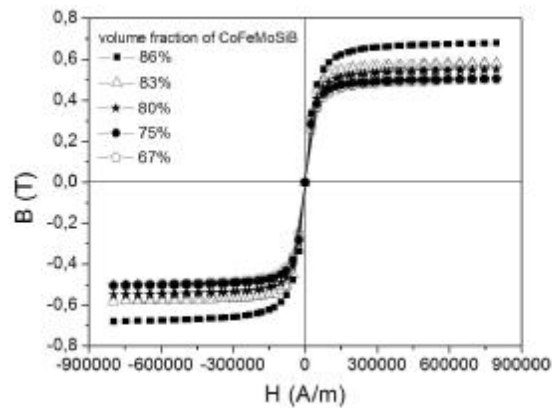


Fig. 9. Hysteresis loops of the SILAME nanocrystalline composite materials with varying volume fraction of nanocrystalline powder

The highest coercive area value was characteristic for the composite with the volume fraction of nanocrystalline powder 86%. Its lowest value was revealed for the composite with the 75% volume fraction (Fig. 9).

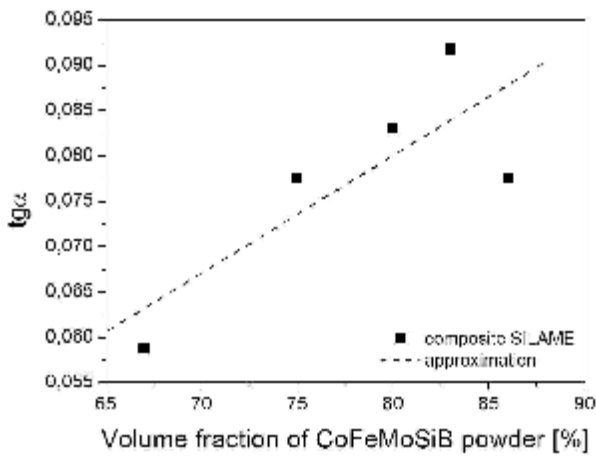


Fig. 3. Tangent of the primary magnetization curve inclination angle versus the volume fraction of nanocrystalline powder CoFeMoSiB in the SILAME type composite: Approximation:  $y=a+bx$ ,  $a=0,024$ ,  $b=0,0013$ ,  $R=80,1$

Table 3

Magnetic properties of the SILAME type composites

Volume fraction of metallic powder CoFeMoSiB [%]	$\rho_{comp}$ [g/cm <sup>3</sup> ]	$B_s$ [T]	$H_C$ [A/m]	$B_R$ [T]	$H_{max}$ [kA/m]
86	6,83	0,73	134,5	0,0014	800
83	6,67	0,68	107,8	0,0013	
80	6,44	0,67	116,1	0,0013	
75	6,11	0,63	54,6	0,0397	
67	5,54	0,50	69,4	0,0303	

Tests of magnetic properties revealed that along with the growing the volume fraction of nanocrystalline powder CoFeMoSiB in the composite the inclination angle of the primary magnetization curve grows also (Fig. 10).

Further observations confirmed that other magnetic properties and the hysteresis loop shape indicate that the magnetic properties deteriorate along with the decreasing the volume fraction of nanocrystalline metallic powder in the composite (Fig. 9).

**Conclusions.** On the basis on results of investigations of magnetic properties of the powder material, it was found out that compared to the magnetic properties of the amorphous ribbon and powder obtained from ribbons in high energy ball milling as their both precursor, the hot pressing process deteriorates their magnetically soft properties.

On the basis on analysis of diffraction patterns and using Scherrer's relationship (4) the Co-a and Co-b grains size was calculated, whose dimensions grow in this case along with the hot pressing temperature decrease, but probably the

calculated peaks include the background form amorphous phase and the results are not binding.

The analysis of the magnetic properties test results of the nanocrystalline composite material revealed that the soft magnetic properties of the composite are dependant on the metallic powder ratio in the composite, which improve with the increase of the  $Co_{68}Fe_4Mo_1Si_{13,5}B_{13,5}$  powder ratio.

The mechanical properties test results of the composites reveal the significant effect of the  $Co_{68}Fe_4Mo_1Si_{13,5}B_{13,5}$  powder ratio on the mechanical properties of the composite, which deteriorate along with the decreasing powder ratio.

**Acknowledgements.** The authors are very grateful to dr. Anna Dolata-Grosz from Department of Metal Alloy and Composites of Technology of Silesian University of Technology for performing hot pressing of metallic powders.

## References

1. Miguel C., Zhukov A., Del Val J.J., Gonzalez J. Coercivity and induced magnetic anisotropy by stress and/or field annealing in Fe- and Co- based (Finemet-type) amorphous alloys // Journal of Magnetism and Magnetic Materials 294 (2005) pp. 245–251.
2. Nowosielski R., Griner S. Shielding of electromagnetic fields by mono- and multi-layer fabrics made of metallic glasses with Fe and Co matrix // Journal of Achievements in Materials and Manufacturing Engineering 20 (2007) pp. 45–54.
3. Lesz S., Nowosielski R., Zajdel A., Kostrubiec B., Stokłosa Z. Structure and magnetic properties of the amorphous  $Co_{80}Si_9B_{11}$  alloy // Journal of Achievements in Materials and Manufacturing Engineering 18 (2006) pp. 155–158.
4. Moya J., Cremaschi V., Silva F.C.S., Knobel M., Sirkin H. Influence of the heat treatment method on magnetic and mechanical properties of the  $Fe_{73,5}Si_{13,5}B_9Nb_3Cu_1$  alloy // Journal of Magnetism and Magnetic Materials 226-230 (2001) pp. 522-1523.
5. Gutiérrez J., Barandiarán J.M., Minguez P., Kaczowski Z., Ruuskanen P., Vlasák G., Svec P., Duhaj P. // Influence of heat treatment on the magnetic and piezomagnetic properties of amorphous and nanocrystalline  $Fe_{64}Ni_{10}Nb_3Cu_1Si_{13}B_9$  alloy strips, Sensors and Actuators A 106 (2003) 69–72.
6. Iwami Y., Okazaki Y., Saito A. Unique stress-magnetization change of Co-based amorphous ribbon due to magnetic field heat treatment // Journal of Magnetism and Magnetic Materials 254–255 (2003) pp. 127–129.
7. Saage G., Roth S., Eckert J., Schultz L. // Low magnetostriction crystalline ribbons prepared by melt spinning and reactive annealing // Journal of Magnetism and Magnetic Materials 254–255 (2003) pp. 26–28.
8. Yapp R., Watts B.E., Leccabue F. // Rapid solidification of Fe-Cr-Si-B alloys by melt spinning, Materials Science and Engineering A304–306 (2001) pp. 1008–1010.
9. Degmová J., Tóth I., Bednarčík J., Kollár P. The influence of ball-milling on structural and magnetic properties of Co-based powders, Czechoslovak Journal of Physics 55 (2005) No. 7, pp. 791-801
10. Gramatyka P., Kolano-Burian A., Kolano R., Polak M. Nanocrystalline iron based powder cores for high

frequency applications // Journal of Achievements in Materials and Manufacturing Engineering 16 (2006) pp. 99-102.

11. *Moumeni H., Alleg S., Greneche J.M.* Structural properties of Fe<sub>50</sub>Co<sub>50</sub> nanostructured powder prepared by mechanical alloying, Journal of Alloys and Compounds 386 (2005) pp. 12-19.

12. *Konieczny J., Dobrzański L. A., Frąckowiak J. E.* Structure and magnetic properties of powder HITPERM materia // Archives of Materials Science and Engineering 28 (2007) pp. 156-164.

13. *Kim Yoon B., Jang D.H., Seok H.K., Kim K.Y.* Fabrication of Fe-Si-B based amorphous powder cores by cold pressing and their magnetic properties // Materials Science and Engineering A 449-451 (2007) pp. 389-393.

14. *Gramatyka P., Nowosielski R., Sakiewicz P.* Magnetic properties of polymer bonded nanocrystalline powder, Journal of Achievements in Materials and Manufacturing Engineering 20 (2007) pp. 115-118.

15. *Gramatyka P., Kolano-Burian A., Kolano R., Polak M.* Nanocrystalline iron based powder cores for high frequency applications // Journal of Achievements in Materials and Manufacturing Engineering 18 (2006) pp. 99-102.

16. *Nuetzel D., Rieger G., Wecker J., Petzold J., Mueller M.* Journal of Magnetism and Magnetic Materials, 196-197 (1999) pp. 323-326.

17. *Muller M., Novy A., Brunner M., Hilzinger R.* Journal of Magnetism and Magnetic Materials, 196-197 (1999) p. 357

18. *Karttunen M., Ruuskanen P.* Materials Science Forum, vol. 269-272 (1998) pp. 849-852.

19. *Ando S., Mine Y., Takashima K., Itoh S., Tonda H.* Journal of Materials Processing Technology, 85 (1999) pp.142-145.

20. *Heptner H., Stroppe H.* Magnetische und magnetoinduktive Werkstoffprüfung, Wydawnictwo „Śląsk“ 1972.

21. *Perov N.S., Radkovskaya A.A., Antonov A.S., Usov N.A., Baranov S.A., Larin V.S., Torcunov A.V.* Journal of Magnetism and Magnetic Materials., 196-197 (1999), pp. 385-388.

22. *Bojarski Z., Łągiewka E.* Structural X-ray analysis, University of Silesia Publishing House, Katowice 1995.

23. *Suryanarayana C.* Mechanical alloying and milling, Progress in Materials Science 46 (2001) pp. 1-184

20.05.07

*Я. Конієчни, Л. Добжанський*

**Структура і властивості нанокристалічних композитних матеріалів**

*Політехніка сілезька, Глівіце,  
Польща*

*Наведені результати дослідження нанокристалічних композитних матеріалів. Властивості магнітного композиційного матеріалу порівнювалися з магнітними властивостями осердь з нанокристалічних металічних смуг і металевих порошоків, спресованих у гарячому стані. Встановлено, що порошоків і композитні магнітні осердя мають дещо гірші магнітні властивості, ніж осердя з нанокристалічних смуг. Зроблена спроба пояснити такий ефект і дослідити вплив структури металічних смуг і грануляції порошку та його форми на властивості композитних матеріалів.*

21 01 01 2007

Національний авіаційний університет

Міжнародна науково-технічна конференція  
**СУЧАСНІ ПРОБЛЕМИ МАШИНОЗНАВСТВА**

Присвячена 75-річчю з дня заснування кафедри машинознавства

23 — 25 червня 2008 року

м. Київ, Україна

**Тематика конференції:**

Матеріалознавство

Сучасні технологічні процеси зміцнення та відновлення деталей машин

Трибологія

Механіка матеріалів і конструкцій

Актуальні проблеми якості та контролю в машинобудуванні

**Адреса Оргкомітету:**

Національний авіаційний університет, корп. 2, к. 306

просп. Космонавта Комарова, 1

м. Київ-58, 03680

Телю/факс: (044) 406-77-73; 497-51-28;

E-mail: [ptznau@ukr.net](mailto:ptznau@ukr.net)